

# Revisiting universality of the liquid-gas critical point in 2D

Max Yarmolinsky and Anatoly Kuklov

<sup>1</sup> *Department of Engineering & Physics, CSI, and the Graduate Center of CUNY, New York.*

(Dated: March 2, 2017)

Critical point of liquid-gas (LG) transition does not conform with the paradigm of spontaneous symmetry breaking because there is no broken symmetry in both phases. This stimulated the ongoing debate about the nature of the universality class of the transition – lasting since the creation of the theory of scaling. We revisit the conjecture that the LG criticality is that of the Ising model. Large scale Monte Carlo simulations of the LG criticality in 2D free space in combination with the numerical flowgram method give the critical indices agreeing with the Onsager values within the error of 1%. The related problem about the role of higher order odd terms in the (real)  $\varphi^4$  field model is addressed too. The scaling dimension of the  $\varphi^5$  term at criticality is shown to be the same as of the linear one  $\varphi$ . We suggest that the role of all higher order odd terms is simply in generating the linear field operator at the criticality.

PACS numbers: 05.50.+q, 75.10.-b

## I. INTRODUCTION

The liquid-gas phase transition is characterized by latent heat which vanishes at one point of the phase diagram – the critical point. Within the mean field approach, the LG coexistence curve is well described by the celebrated van der Waals equation where the role of the order parameter is played by the difference in densities of liquid and gas (see in Ref.<sup>1</sup>). Formally speaking, however, neither liquid nor gas can be characterized by symmetry breaking order parameter simply because there is no order in both phases.

Absence of any underlying symmetry breaking raises the question about the universality of the transition at the critical point. The standard conjecture is that this transition belongs to the  $Z_2$  universality class, that is, of the Ising transition (see in Refs.<sup>1-3</sup>). This question have a straightforward answer for the lattice gas where a direct mapping to Ising model exists<sup>4</sup>. It is formally possible to consider a free space fluid on a lattice with the spacing being much smaller than any typical distance determining interaction. In this case the lattice and free space models should be equivalent. Thus, in general, no underlying  $Z_2$  symmetry can be found in such a lattice. Accordingly, lattice models explicitly violating  $Z_2$  symmetry have been considered<sup>5</sup>. It was further suggested that the asymmetry does not change the  $Z_2$  universality of the LG criticality, and its role is reduced to mixing of the primary scaling operators which results in the non-analytical corrections to the position of the critical point<sup>3,6,7</sup>.

The conjecture that LG criticality is  $Z_2$  is closely related to the question about the role of higher order odd terms in the field theory. As shown in Ref.<sup>8</sup>, the LG transition characterized by quite generic two-body interactions in free space can be mapped on a field theory of a continuous scalar field  $\varphi$  with some effective Hamiltonian which, in addition to even terms  $(\vec{\nabla}\varphi)^2, \varphi^2, \varphi^4, \dots$ , contains odd ones  $\varphi^1, \varphi^3, \varphi^5, \varphi^7, \dots$ . Thus, there is a possibility that higher order odd terms  $\varphi^5, \varphi^7, \dots$  change

the universality (the term  $\varphi^3$  can be eliminated by a uniform shift  $\varphi \rightarrow \varphi + \varphi_0$  with  $\varphi_0$  being some constant)<sup>9</sup>. The analysis<sup>10</sup> based on the renormalization group (RG) approach finds that there is a novel fixed point in dimensions  $d = 10/3$  induced by the term  $\varphi^5$ , provided,  $\varphi^1$  and  $\varphi^3$  are tuned to zero. This result, however, was challenged by the analysis<sup>11</sup> based on the  $\varepsilon$ -expansion around  $d = 4$  showing that all odd operators of higher order are strongly irrelevant at the symmetric fixed point, so that this point is stable with respect to the odd perturbations.

It is important to note that the argument<sup>11</sup> cannot be used in 2D. Thus, the question about the role of the higher odd terms in 2D remains open. More recently, the analytical solution for the critical exponents of 3D LG transition has been found under quite general assumptions<sup>12</sup>. These exponents turn out to be different from the values obtained numerically. The same method can also be used in 2D and it gives the exponents which are different from the Onsager values as well<sup>13</sup>. This revitalizes the possibility that the LG criticality is not of  $Z_2$  class.

The situation with the experiment is not that conclusive. Some early experiments aimed at measuring the critical indices have claimed significant deviations from the 3D Ising universality<sup>14,15</sup>, while others<sup>16,17</sup> find an acceptable agreement with the Ising universality, provided the fitting procedure included subcritical corrections (with several adjustable parameters). The main problem turns out to be due to the gravity which does not allow to approach the critical point close enough so that the corrections can be ignored. The experiments in microgravity (see in Ref.<sup>18</sup>) didn't improve the situation much.

The LG critical point has been addressed by direct Monte Carlo simulations. In Ref.<sup>19</sup> the analysis of 2D Lennard-Jones fluid has been carried out within the hypothesis of the mixing<sup>3,6,7</sup>, and it has been concluded that the universality of the transition is consistent with the  $Z_2$  class. However, the maximum size simulated in this work allowed to include only about 400 particles on

average, with two relatively small sizes of the simulation box used. Under this condition the applicability of the finite-size scaling (FSS) analysis becomes questionable. The same approach has been used in 3D<sup>20</sup> with the conclusion that the 3D LG critical point belongs to the  $Z_2$  class. The role of corrections to scaling turns out to be much more important in 3D. This, in particular, lead to inconsistent values of the  $\nu$  exponent deduced from different quantities. Thus, the accuracy of the numerical results do not allow to exclude the non-Ising universality<sup>12</sup> with high confidence.

Monte Carlo simulations have been also conducted for the model interaction potential – the square well in 3D in Ref.<sup>21</sup> (see also references there). The analysis was carried out for a set of box sizes from 6 to 18 hard core radii, and the conclusion was reached that the universality of the critical point is consistent with the  $Z_2$  class. Later, however, a different result has been obtained for Lennard-Jones potential<sup>22</sup> – the critical exponent  $\nu$  was not consistent with the Ising class. The LG criticality has been also addressed in a series of papers<sup>23–25</sup>, where both the critical exponent  $\nu$  and the critical histogram were found to be consistent with those of the 3D Ising. [At this point, however, we should notice that the accuracy in the  $\nu$ -exponent value does not allow to exclude the non-Ising universality<sup>12</sup>]. The approach based on molecular dynamics has been utilized in Ref.<sup>26</sup> and significantly larger sizes have been simulated with the conclusion that the LG criticality in 3D is of Ising type.

It is important to note that the methods used to evaluate the critical exponents in Refs.<sup>19–22,26</sup> are strongly dependent on the choice of the values of the critical temperature  $T_c$  and pressure  $P_c$  (or density). This introduces significant uncertainties in the exponents. In 3D the corrections to scaling must also be included. Thus, the fits become multi-parametric which introduces even larger errors.

Here we suggest a different approach – based on the so called *numerical flowgram* first introduced in Ref.<sup>27</sup> and further developed in Ref.<sup>28</sup>. Within this method a position of the critical point stems as a byproduct of tuning a system into criticality with the help of the Binder cumulants. Thus, error in the critical exponents is given essentially by the error of the Binder cumulant only. We apply this method to the LG critical point in 2D. The role of the  $\varphi^5$  term at the critical point of the field model  $\varphi^4$  in 2D is addressed as well. The outcome of our large scale simulations allows to conclude with high certainty that the 2D LG criticality does belong to the Ising class because the resulting critical exponents coincide with those of the Ising model within error bar of 1%. Using the same method we have determined the scaling dimension of the  $\phi^5$  term in the  $\varphi^4$  model and have found that it coincides with that of the linear term (within 1% of the error). This allows to conjecture that all higher order odd terms are simply equivalent to the linear one  $\varphi$  at the critical point.

## II. CRITICALITY WITH THE $\varphi^5$ TERM

The proposal<sup>10</sup> of the asymmetric fixed point is based on the assumption that the operator  $Q_5 = \int d^d x \varphi^5$  (present in the  $\varphi^4$  field model) is relevant at the symmetric fixed point in  $d < 10/3$ -dimensional space. Then, the symmetric point may become unstable and the system finds another (asymmetric) fixed point characterized by critical indices different from those of the Ising model<sup>10</sup>. The alternative view based on the  $\epsilon$ -expansion around  $d = 4$  renders  $Q_5$  and all higher terms as (dangerously) irrelevant<sup>11</sup>. [This argument, however, cannot be used in 2D].

Here we will discuss the results of the simulations of the standard model of real field  $\varphi$  in 2D with the  $Q_5$  term. Far from the criticality, this term causes system instability which needs to be cut off by a higher order even terms, say,  $\sim \varphi^6$ . In reality, any even positive term higher than  $\sim \varphi^4$  is sufficient. Within the paradigm of universality, the critical behavior of the  $Q_5$  should not be affected by this choice. To simplify the simulations we have selected the model with the potential energy  $\sim g_4 \varphi^4 - \ln(1 + g_5 \varphi^5)$ . Then, the partition function defined on a square lattice becomes

$$Z = \int D\varphi \exp(-H) \prod_i (1 + g_5 \varphi_i^5), \quad (1)$$

with

$$H = -t \sum_{\langle ij \rangle} \varphi_i \varphi_j + \sum_i [a \varphi_i^2 + g_4 \varphi_i^4], \quad (2)$$

where the field  $\varphi_i$  is defined at a site  $i$  of the lattice, and the summation  $\sum_{\langle ij \rangle}$  runs over nearest neighbor sites; and  $t > 0, a > 0, g_4 > 0, g_5 > 0$  are parameters. We have chosen  $a = g_4 = 1$  and have tuned the system into the criticality by adjusting  $t$  to some critical value  $t = t_c$  and  $g_5 = g_c$ .

It is important to note that we have found no critical point at any finite value of  $g_5$  – the correlation length was finite for any  $g_5 \sim 1$  and below. Thus, we conclude that there is only one critical point – with  $g_5 = g_c = 0$ . Then the question should be answered about the scaling dimension of the  $g_5$ -term. This can be achieved by observing the divergence of the correlation length  $\xi \sim g_5^{-\mu_5}$  with some exponent  $\mu_5 > 0$  as  $g_5 \rightarrow 0$  provided  $t = t_c$ . Jumping ahead, we have found that  $\mu_5$  coincides with the Onsager value  $\mu = 8/15$  (within 1% of the total error).

### A. Critical behavior at $g_5 = 0$ by the flowgram method

The idea of the flowgram method<sup>27,28</sup> is based on constructing the finite size scaling (FSS) flow by tuning a parameter (say,  $t$ ) to have a certain value of some Binder cumulant  $U_B$ <sup>29</sup> within its critical range and, then, determining how any quantity  $Q$  of interest plotted vs  $U_B$

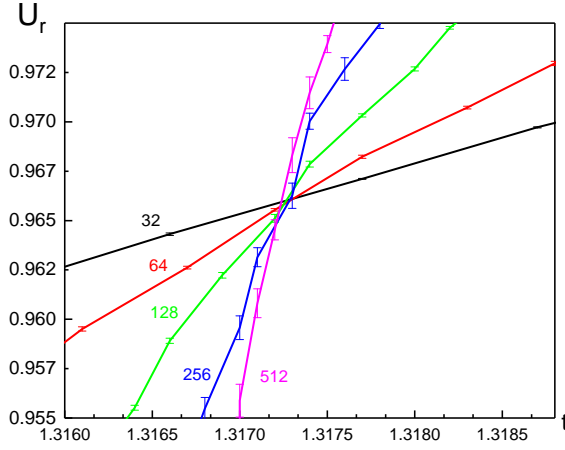


FIG. 1: (Color online)  $U_r$  vs  $t$  for various  $L$  shown close to each curve. This crossing point corresponds to  $U_B = 0.965$  and it determines  $t_c = 1.3173 \pm 0.0003$  (for  $g_4 = 1$ ,  $a = 1$ ,  $g_5 = 0$  in Eqs.(1,2)).

scales within FSS. If  $U_B$  is kept in the critical range for large enough  $L$ , the plot of  $Q$  versus  $U_B$  can be represented by some universal function multiplied by the factor  $L^\Delta$  with some exponent  $\Delta$  determining scaling dimension of  $Q$ .

More specifically, far from the criticality  $U_B$  takes some fixed values, say,  $U_B = B_0$  in the disordered phase and  $U_B = B_1$  in the ordered phase. At the critical point,  $t = t_c$  (and  $g_5 = 0$ ), it takes a value  $U_B = B_c$  independent of the system size  $L$  as long as  $L \rightarrow \infty$  and such that  $B_0 < B_c < B_1$  (where for the sake of argument we assume  $B_1 > B_0$ ). It is important to note that for any finite  $L$  the function  $U_B(t)$  changes smoothly from  $B_0$  to  $B_1$  as  $t$  passes from  $t < t_c$  to  $t > t_c$ . However, as  $L$  is taken larger and larger, the domain  $\delta t$  around  $t = t_c$  over which this change happens becomes smaller and smaller. Thus, in the thermo-limit ( $L \rightarrow \infty$ ) the cumulant exhibits a jump from  $B_0$  to  $B_1$  at exactly  $t = t_c$  because the domain  $\delta t$  shrinks to zero in accordance with the FSS behavior  $\delta t \sim L^{-1/\nu}$ . This allows to approach the critical point by tuning  $U_B$  to the critical range  $B_0 < U_B < B_1$  in the progression of growing sizes  $L$ . Accordingly, the system is always in the critical range of  $U_B$  (and of any other scaling quantity). In particular, the family of curves  $dU_B/dt$  vs  $U_B$  for various  $L$  must be self-similar for large enough  $L$  because  $dU_B/dt \approx (B_1 - B_0)/\delta t \propto L^{1/\nu}$ . Thus, constructing such a family and then rescaling them into a single master curve by a scaling factor  $\lambda(L)$  gives the exponent  $\nu$  by plotting  $\ln \lambda$  vs  $\ln L$ . Similarly, other exponents can be found by choosing the appropriate quantity  $Q$  to plot it vs  $U_B$  and to perform the rescaling of the family of the curves (for various  $L$ ) into a single master curve. Clearly, within this approach the value of  $t_c$  plays no explicit role in the fitting procedure with only one fitting parameter – the critical exponent.

In order to determine the  $\nu$  exponent (of the correlation length  $\xi \sim |t - t_c|^{-\nu}$ ) we have chosen the following Binder

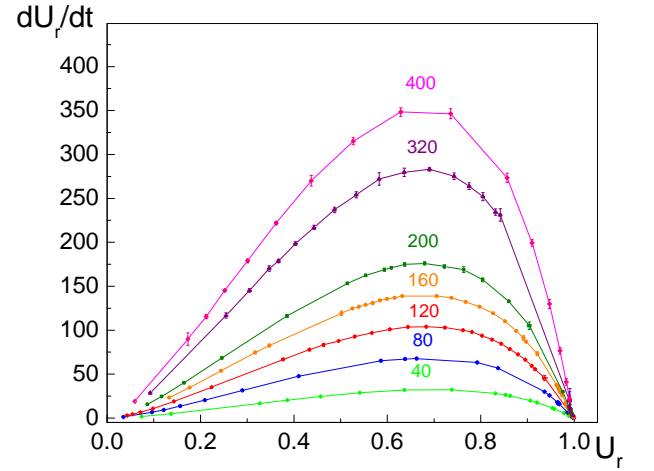


FIG. 2: (Color online) Monte Carlo results for  $dU_r/dt$  vs  $U_r$  as defined in Eq.(7) for several system sizes  $L$  shown close to each curve. Lines are guides to eye.

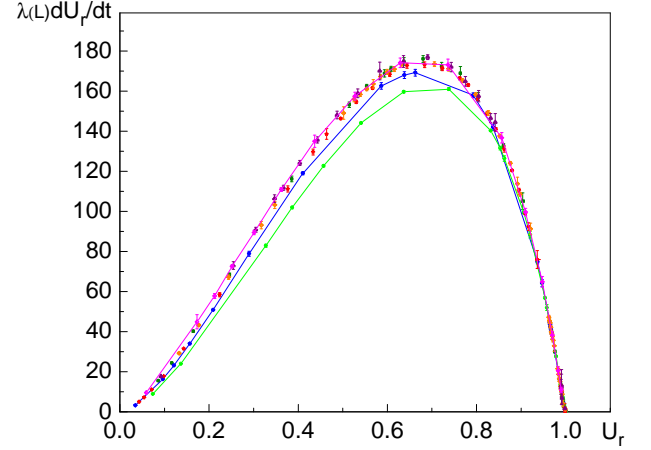


FIG. 3: (Color online) Rescaled data shown in Fig. 2 with  $\lambda(L) = (200/L)^{1/\nu}$ ,  $\nu = 1$ . The overall statistical error of the data is  $\sim 1 - 2\%$ .

cumulant

$$U_r(t, L) = \frac{\langle r^2 \rangle_G}{r_L^2}, \quad r_L^2 = \sum_{\vec{r}} \vec{r}^2 / L^d \propto L^2, \quad (3)$$

where  $\langle r^2 \rangle_G = \sum_{\vec{r}} G(\vec{r}) \vec{r}^2 / \sum_{\vec{r}} G(\vec{r})$ , with  $G(\vec{r})$  denoting the correlator  $\langle \varphi(\vec{r}) \varphi(0) \rangle$  taken at two points in 2D space separated by the vector  $\vec{r}$ ; and  $\langle \dots \rangle$  defines the averaging with respect to the partition function(1). To demonstrate that  $U_r$  is a scale invariant quantity at the critical point, we have analyzed its behavior vs  $t$  for various sizes. Fig. 1 shows the crossing point of  $U_r$  at  $t = t_c$ . By the definition, Eq.(3),  $U_r \rightarrow 0$  (as  $L \rightarrow \infty$ ) in the disordered phase (where the correlation length is  $\sim \mathcal{O}(1)$ ) and  $U_r = 1$  in the ordered phase where the coherence length reaches the system size  $L$ . Thus, formally speaking, any value in the range  $0 < U_r < 1$  belongs to the critical range of  $U_r$ , and tuning  $t$  in such a way that  $U_r$  stays within the critical range for each simulated  $L$  guarantees that  $t \rightarrow t_c$ . In reality, for practical purposes of achieving better accuracy in the critical exponent we have found that it is

reasonable to tune  $U_r$  into the region where  $dU_r/dt$  vs  $U_r$  reaches its maximum. Fig. 2 shows that this range corresponds to the domain  $0.5 < U_r < 0.8$ .

We have conducted simulations by the Worm Algorithm<sup>30</sup> using the high temperature expansion of the partition function in the term  $\sim t$ . Specifically, at each bond the factor  $\exp(t\varphi_i\varphi_j)$  is expanded and then the result is integrated out with respect to the field. The resulting partition function (1) is represented in terms of the powers and coefficients of the expansion as

$$Z = \sum_{\{N_{ij}\}, \{n_i\}} \prod_{\langle ij \rangle} \left( \frac{t^{N_{ij}}}{N_{ij}!} \right) \prod_i [S(C_i) g_5^{n_i}], \quad (4)$$

where  $N_{ij} = 0, 1, 2, \dots, \infty$  are integers defined at bonds between neighboring sites  $i$  and  $j$ ;  $n_i = 0, 1$  are defined at sites, and

$$S(C) = \int_{-\infty}^{\infty} d\varphi \varphi^C \exp(-a\varphi^2 - g_4\varphi^4), \quad (5)$$

with

$$C_i = \sum_{j=\langle i \rangle} N_{ij} + 5n_i, \quad (6)$$

where  $\sum_{j=\langle i \rangle}$  denotes summation over bonds connected to the site  $i$ .

Here we first discuss the case  $g_5 = 0$  so that  $n_i = 0$  at all sites. Thus, the configurational space is completely determined by the integers  $N_{ij}$  which form closed non-oriented loops. Evaluation of the correlator corresponds to having one loop with two open ends<sup>30</sup>. In this space,  $U_r$  can be constructed as the histogram of the square of the distance  $\bar{r}^2$  between two open ends which represent two random walkers. Accordingly  $dU_r/dt$  can be found as

$$t \frac{dU_r}{dt} = \sum_{\langle ij \rangle} [\langle N_{ij} \bar{r}^2 \rangle_G - \langle N_{ij} \rangle_G \langle \bar{r}^2 \rangle_G] \quad (7)$$

following direct differentiation vs  $t$  in the dual representation (4,5,6).

The result of this procedure – the family of graphs  $dU_r/dt$  vs  $U_r$  for various  $L$  is shown in Fig. 2. The master curve obtained by the vertical rescaling of the data with the exponent  $\nu = 1$  is shown in Fig. 3. The lines connecting the data points for  $L = 40, 80$  are shown in order to emphasize that at these sizes the sub dominant term is still visibly significant so that these data points do not collapse into the master curve. The line for  $L = 400$  is also shown to indicate that all higher sizes  $L = 120, 160, 200, 320, 400$  belong to the master curve within the error 1-2%.

At finite  $g_5$  the structure of the configurational space changes – there are loops which are not closed. The general condition (6) indicates that whenever  $n_i = 1$  at a site  $i$ , there is an odd total number of the integers  $N_{ij}$  at the bonds connecting this site with its neighbors  $j$ .

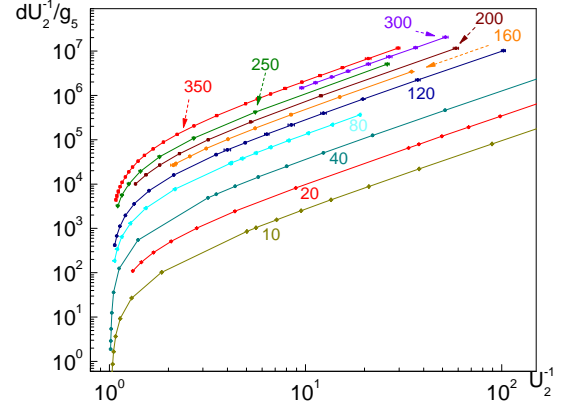


FIG. 4: (Color online) Monte Carlo results for  $dU_2^{-1}/dg_5$  vs  $U_2^{-1}$  for sizes  $L$  shown close to each curve.

## B. Critical behavior at finite $g_5$

Ising critical behavior is characterized by two primary fields  $\sim \varphi^2$  and  $\sim \varphi$  with the corresponding "charges"  $\tau \sim t - t_c$  and  $h$ . In the space  $(\tau, h)$  the divergence of the correlation length  $\xi$  along the line  $h = 0$  is characterized by  $\xi \sim \tau^{-\nu} \rightarrow \infty$  and by  $\xi \sim h^{-\mu} \rightarrow \infty$  along  $\tau = 0$ , with the Onsager exponents  $\nu = 1$ ,  $\mu = 5/18$ . According to the FSS, once  $\xi$  reaches the system size  $L$ , the role of  $\xi$  is taken over by  $L$ . In the previous section we have explored the first property and have shown that the scaling dimension of  $\tau$  is  $1/\nu$  with  $\nu = 1$ . In order to observe the divergence along the second line one should select  $t = t_c \approx 1.3173$  as determined from the previous procedure for largest sizes and to apply the frowgram method – now at finite  $h$ . In this case plotting  $dU_B/dh$  vs  $U_B$  for various  $L$  and constructing the master curve by rescaling  $dU_B/dh$  into a single master curve by some factor  $\lambda(L)$  for each  $L$  will give the  $\mu$  exponent.

The above logic can be exploited in order to determine scaling dimensions of higher odd terms in the action. Here we will be concerned with the term  $\sim \varphi^5$  as the most possibly relevant one – as suggested in Ref.<sup>10</sup>. We determine the corresponding critical index  $\mu_5$  from the rescaling procedure of the graphs  $dU_B/dg_5$  versus  $U_B$  for various  $L$ .

Here, though, we have to change the type of the Binder cumulant. At finite  $g_5$  (or in the presence of any other odd term) using the cumulant  $U_r$ , Eq.(3), is not convenient because the number of open loops is now a dynamical variable. Instead we use

$$U_2 = \frac{\langle \psi \rangle^2}{\langle \psi^2 \rangle}, \quad \psi \sim \sum_i \varphi_i^5. \quad (8)$$

Clearly,  $U_2 = 0$  at  $g_5 = 0$  (simply because  $\langle \varphi_i^5 \rangle = 0$ ) and  $U_2 = 1$  far away from the critical point – where fluctuations are suppressed.

It is possible to express  $U_2$  in terms of the dual variable  $N_5 = \sum_i n_i$ , where  $n_i$  has been introduced in the

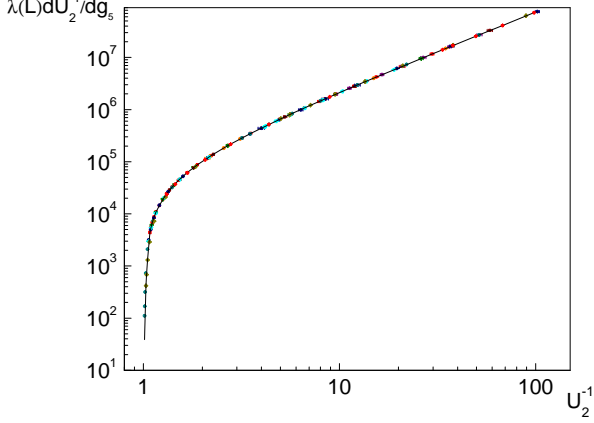


FIG. 5: (Color online) The master curve obtained by "vertical" rescaling of the curves from Fig. 4 by the factor  $\lambda(L) \sim L^{1/\mu_5}$  to match the data for  $L = 350$ . The log-log plot of  $\lambda$  vs  $L$  gives  $\mu_5 = 0.533 \pm 0.005$  consistent with the 2D Ising value  $\mu = 8/15$ .

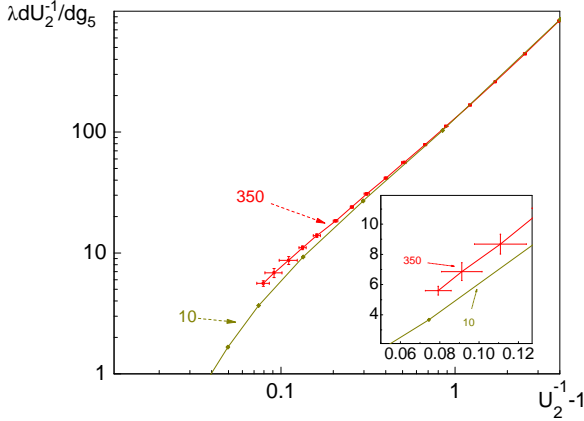


FIG. 6: (Color online) Deviation from the scaling. Two curves,  $L = 10, 350$ , from the data Fig. 5 are shown in the domain where deviations from scaling are significantly higher than the statistical error of 1% (about 15%). Inset: More detailed view on the linear scale.

dual representation (4,5,6) of the original system (1,2). Specifically, we introduce  $U_2 = (dZ/dg_5)^2/[Zd^2Z/dg_5]$ . Using the dual form (4) of  $Z$ , this gives

$$U_2 = \frac{\langle N_5 \rangle^2}{\langle N_5(N_5 - 1) \rangle}, \quad N_5 \equiv \sum_i n_i. \quad (9)$$

Here we used the relations  $d \ln Z/dg_5 = g_5^{-1} \langle N_5 \rangle$  and  $d^2 Z/dg_5^2 = g_5^{-2} \langle N_5(N_5 - 1) \rangle$ . It is useful to notice that in terms of the original representation (1),  $\langle N_5 \rangle = g_5 \langle \psi \rangle$  where  $\psi \equiv \sum_i \frac{\varphi_i^5}{1+g_5 \varphi_i^5}$ . In the limit  $g_5 \rightarrow 0$  (relevant to our consideration) this transforms into  $\psi = \sum_i \varphi_i^5$ . Accordingly,  $\langle N_5(N_5 - 1) \rangle = g_5^2 [\langle \psi^2 \rangle - \sum_i \langle \varphi_i^{10} \rangle / (1 + g_5 \varphi_i^5)^2] \rightarrow g_5^2 \langle \psi^2 \rangle$  (because the term  $\sim \langle \psi^2 \rangle$  has the extra factor  $L^2$  with respect to  $\sim \sum_i \langle \varphi_i^{10} \rangle$ ).

The variation of  $U_2$  versus  $g_5$  from 0 to 1 occurs over the domain shrinking with  $L \rightarrow \infty$  as the power

$\sim L^{-1/\mu_5}$ ,  $\mu_5 > 0$ . As follows from Eqs.(4), the derivative  $dU_2/dg_5$  can be expressed in terms of averages of powers of  $N_5$  with the help of the general relation for the derivative  $d\langle Q \rangle/dg_5 = g_5^{-1}[\langle QN_5 \rangle - \langle Q \rangle \langle N_5 \rangle]$  of any quantity  $Q$ . The result of the simulations are presented in Fig. 4.

The family of curves, Fig. 4, can be collapsed to a single master curve, Fig. 5, by the scale factor  $\lambda(L) \sim L^{-1/\mu_5}$  with the exponent  $\mu_5 = 0.533 \pm 0.005$ . This exponent turns out to be consistent with the 2D Ising value  $\mu = 8/15$  within 1% of the combined error – systematic and statistical. It is important to note that the range of  $\lambda$  extends over almost 3 orders of magnitude. In order to emphasize the quality of the collapse, we have included the plot Fig. 6 showing two sizes  $L = 10, 350$  rescaled to each other within a narrow range of  $U_2^{-1} - 1$ . A visible deviation from scaling starts for  $U_2^{-1} - 1 < 1$ .

This concludes our analysis of the role of the symmetry breaking term  $\varphi^5$  in 2D. Within the accuracy of 1% and up to the simulated sizes of  $L = 350$  this term has the same scaling dimension as the linear one  $\varphi$ . Using similar approach, higher odd terms can be considered too.

### III. LG CRITICALITY IN 2D

Above we have discussed the role of higher odd terms in the field theory along the line of the universality paradigm – when a particular form of the action is not important as long as a system is close to the fixed point. The relation of this study to the actual LG criticality stems from the formal mapping of the classical gas to a field theory<sup>8</sup>.

Here we will discuss the LG transition in 2D gas of classical particles by simulating it directly. We choose the simplest interacting potential – the square well. The same flowgram method will be used to determine the critical behavior in this case. The system of classical particles is described by the grand canonical partition function

$$Y = \sum_{N=1}^{\infty} \frac{1}{N!} e^{\tilde{\mu}N} \int d\vec{r}_1 \dots d\vec{r}_N e^{-V}, \quad (10)$$

where  $V = (1/2) \sum_{ij} v(\vec{r}_i - \vec{r}_j)$  is the potential energy of binary interaction (normalized by temperature) between  $N$  particles located at  $\vec{r}_i$ ,  $i = 1, 2, \dots, N$  within the square area  $L^2$ ;  $\tilde{\mu}$  is the chemical potential (normalized by temperature).

The interaction energy between two particles separated by a vector  $\vec{r}$  is taken as the square well potential. That is  $v = \infty$ , if  $r < \sigma$ ;  $v = -\epsilon$ , if  $\sigma \leq r \leq \lambda$  and  $v = 0$ , if  $r > \lambda$ . Here  $\sigma$  and  $\lambda > \sigma$  are the hard and soft core radii, respectively, and  $\epsilon > 0$  characterizes attraction within the soft core shell. Since temperature is absorbed into the definition of  $\epsilon$ , we will be calling  $1/\epsilon$  as "temperature"  $T$  and  $\tilde{\mu}$  as "chemical potential".

The quantities of interest are cumulants of the total number of particles  $N$ , that is,  $\langle N^p \rangle$  with  $p = 1, 2, 3, \dots$

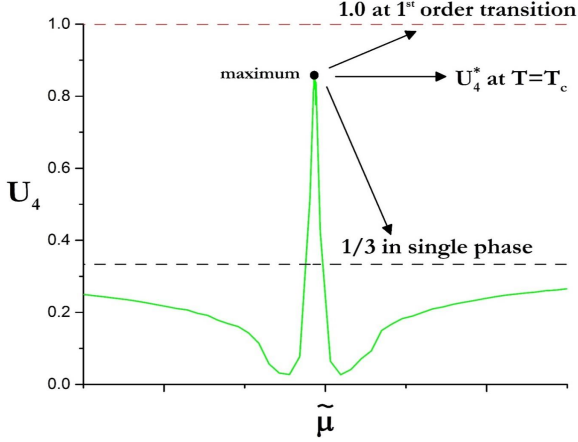


FIG. 7: (Color online) Sketch of the Binder cumulant (11)

In the plane  $(\tilde{\mu}, T)$  there is a line of 1st order phase transition between low and high density phases. This line ends by the critical point at some  $\tilde{\mu} = \mu_c$ ,  $T = T_c$ . One of the significant difficulties in analyzing the LG transition is in finding this point in a controlled manner. Below, we will address this difficulty with the help of the flowgram method which leads to the critical point automatically. For this purpose we consider the following Binder cumulant

$$U_4 = \frac{\langle (N - \langle N \rangle)^2 \rangle^2}{\langle (N - \langle N \rangle)^4 \rangle}, \quad (11)$$

and its derivatives  $dU_4/d\tilde{\mu}$  and  $dU_4/d\epsilon$ . [These derivatives can be expressed in terms of the cumulants  $\langle N^p \rangle$ , with  $p = 2, 3, \dots$  and  $\langle N^p E \rangle$ , where  $E$  is the total energy of the system].

As discussed in Ref.<sup>29</sup>, this cumulant has a specific form: away from the coexistence line it is  $U_4 = 1/3$  in the limit  $L \rightarrow \infty$ . At the coexistence line it has two dips corresponding to the densities of liquid and gas, with the peak in between corresponding to  $U_4 = 1$ . Above the critical point this maximum tends toward the value  $U_4 = 1/3$ . Thus, at the critical point the dips approach each other, with the peak reaching some intermediate value  $1/3 < U_c < 1$ . This value is scale invariant<sup>25</sup>. Fig. 7 illustrates this specific form of the cumulant. In other words, the critical point corresponds to the separatrix of the maximum of  $U_4$  as a function of  $T, \tilde{\mu}$  with respect to  $L \rightarrow \infty$ . This suggests a protocol for finding the critical point: 1. choose some  $T$  and find maximum of  $U_4$  by adjusting  $\tilde{\mu}$  for each size  $L$ ; 2. If this maximum flows toward 1 (toward  $1/3$ ), increase (decrease)  $T$  and repeat the previous step until the flow of  $U_4$  maximum (versus  $L$ ) saturates to some constant value. The result of this procedure is shown in Fig. 8.

Thus, while keeping  $T = T_c$  the FSS can be conducted by tuning  $\tilde{\mu}$  in the vicinity of  $\mu_c$  so that  $U_4$  stays within the critical range  $1/3 < U_4 < U_c$ . Then, plotting  $dU_4/d\tilde{\mu}$  versus  $U_4$  should allow finding the corresponding exponent. There is one complication, though, – a possibility of mixing of the primary operators in  $N$  and  $E$  in *a priori*

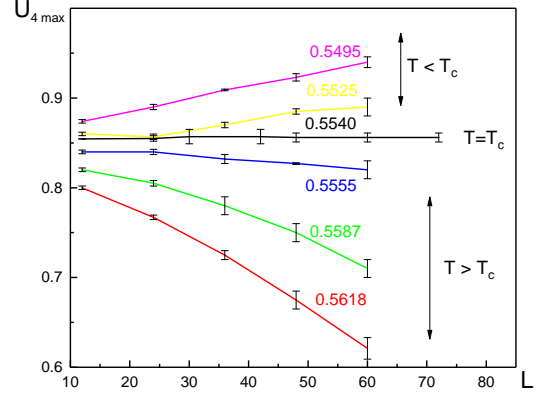


FIG. 8: (Color online) Monte Carlo results of  $U_4$  maximum for several temperatures in regions  $T < T_c$  and  $T > T_c$ . The horizontal line, separatrix, corresponds to  $T_c = 0.5540 \pm 0.0005$  and  $\tilde{\mu} = -3.700 \pm 0.005$ .

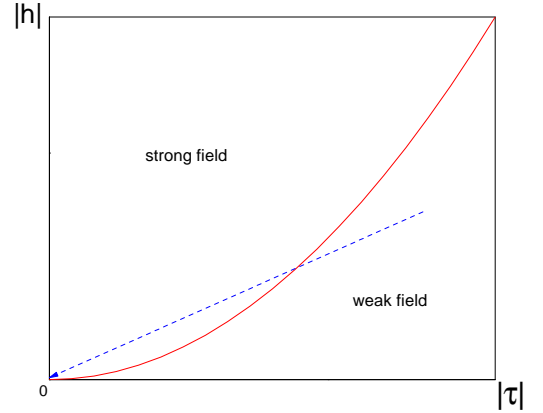


FIG. 9: (Color online) A generic path (dashed line) toward the critical point ( $h = 0$ ,  $\tau = 0$ ) in presence of the mixing effect when scaling dimension  $1/\mu$  of  $h$  is larger than that,  $1/\nu$ , of  $\tau$ . The solid line,  $h^* \sim |\tau|^{\nu/\mu}$  with  $\nu/\mu > 1$ , separates the regions of strong and weak field.

unknown proportions as suggested in Refs.<sup>3,6,7</sup>. Thus, it is not known along which line in the space of the primary scaling operators  $(\tau, h)$  the system approaches criticality, if, say,  $\tilde{\mu}$  is tuned toward  $\mu_c$  while  $T$  is kept at its critical value  $T = T_c$ . It is, however, possible to argue that, generically, the approach to the critical point should proceed along the line where the primary operator with smaller scaling dimension dominates. This argument goes as follows: the critical range can be divided into two parts – of strong and weak field<sup>1</sup>. The separation between the two regions are determined by the relation  $h^* \sim \tau^{\nu/\mu}$  so that at  $|h| > h^*$  the critical singularities are determined by  $h$  rather than by  $\tau \rightarrow 0$ . Thus, if  $\mu < \nu$ , any path  $\tilde{\mu} - \mu_c \sim r_1\tau + r_2h$  toward the critical point  $\tau = 0, h = 0$  with non-zero mixing coefficients  $r_{1,2}$  will belong to the region of strong field close enough to the critical point – as sketched in Fig. 9. Accordingly, conducting the FSS with respect to  $\tilde{\mu}$  will give



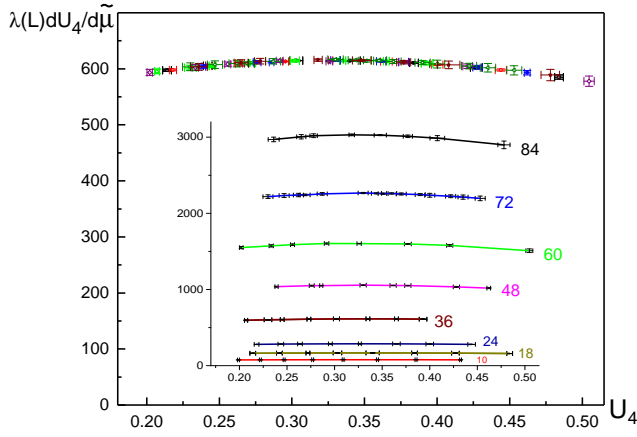


FIG. 10: (Color online) The master curve obtained by "vertical" rescaling of the curves  $dU_4/d\tilde{\mu}$  vs  $U_4$  for sizes  $L = 10, \dots, 84$  by the factor  $\lambda(L)$  to achieve the best collapse. Inset: the original data for sizes shown close to each curve.

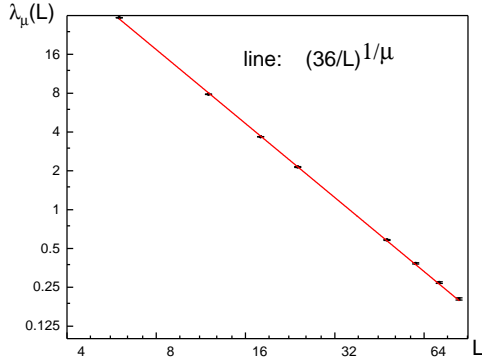


FIG. 11: (Color online) The rescaling factor  $\lambda$  vs  $L$  obtained from the data shown in Fig. 10. The value of the exponent is obtained as  $\mu = 0.532 \pm 0.005$  which is consistent with the Onsager value  $\mu = 8/15$ .

the  $\mu$  exponent. Conversely, if  $\mu > \nu$ , the approach will proceed along a path in the weak field region so that the flowgram method will give the  $\nu$  exponent. The result of the flowgram analysis of  $dU_4/d\tilde{\mu}$  vs  $U_4$  is shown in Fig. 10 with the rescaling factor  $\lambda$  plotted in Fig. 11. As can be seen the resulting exponent  $\mu = 0.532 \pm 0.005$  is consistent with the Ising value  $8/15$  within 1% of the statistical error.

We have also analyzed the compressibility of the system  $\kappa = \langle(N - \langle N \rangle)^2\rangle/L^2$  within the flowgram method, that is, by plotting it vs  $U_4$  in the critical range. The result is presented in Figs. 12,13. The exponent  $(1 - 1/\delta)/\mu = \gamma/\nu = 1.75 \pm 0.05$ , where  $\delta, \gamma$  are the critical exponents (related to each other through the scaling relations), is consistent with the Onsager value  $7/4$ . Thus, the results of our simulations strongly support the con-

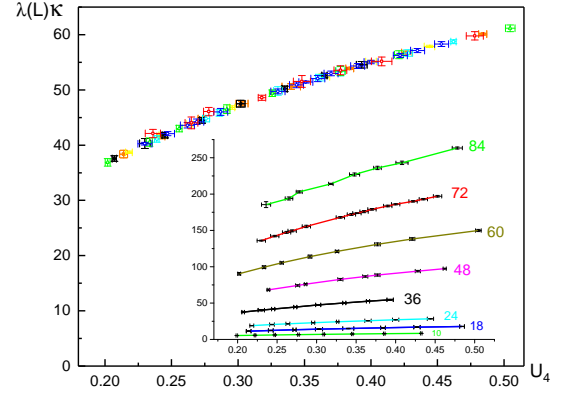


FIG. 12: (Color online) The master curve of the compressibility  $\kappa$  vs  $U_4$  obtained by rescaling of the individual curves for simulated  $L$ . Inset: the original data for each size  $L$  shown close to each curve.

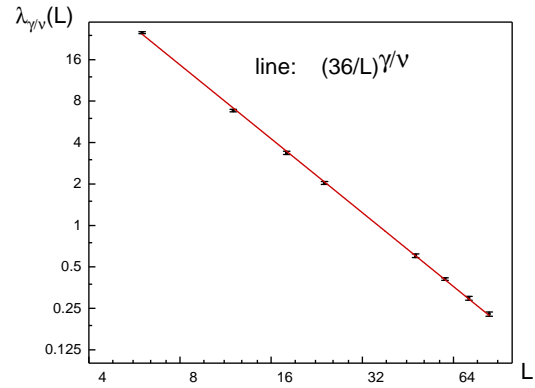


FIG. 13: (Color online) The rescaling factor  $\lambda$  vs  $L$  obtained from the data shown in Fig. 12, with the exponent  $\gamma/\nu = 1.75 \pm 0.01$  consistent with the Onsager value  $\gamma/\nu = 7/4$ .

jecture that the LG criticality in 2D belongs to the Ising class.

#### IV. DISCUSSION

The flowgram method<sup>27,28</sup> is demonstrated to be a universal numerical tool in FSS analysis. Its main advantage is in avoiding numerical fits where accurate knowledge of the position of the critical point is required. This approach has been applied to the field model as well as to the classical gas. The source of errors in this approach is in the values of the Binder cumulant as well as in its derivatives with respect to the scaling parameters. Thus, no error in the critical parameters contributes to the ex-

ponents.

The scaling dimension of the  $\phi^5$  term has been determined to be the same as of the linear term. We conjecture that all odd terms are equivalent to the linear one at the criticality. In simple terms, the mechanism can be illustrated by the following picture. A higher odd term  $\sim \int d^d x \phi^{2n+1}$  with  $n = 2, 3, \dots$  in (2) can be decomposed as  $\phi = \phi_L + \phi_s$  into a long range part  $\phi_L$  and short range fluctuations  $\phi_s$  so that at the criticality the relevant contribution is  $\sim \int d^d x \phi_L \phi_s^{2n}$  where  $\phi_s^{2n}$  can be replaced by a short range contribution which is a non-critical constant.

Here we have also addressed the LG criticality of a classical gas in 2D free space. The analysis is based on applying the flowgram method to the Binder cumulant showing a specific behavior<sup>25</sup>. Our finding is that it is

characterized by Onsager value of the critical exponent  $\mu$ . The same method can be used in 3D. However, the analysis is complicated by the low value of the exponent  $\theta \approx 0.54$  determining correction to scaling. Thus, in order to suppress such corrections within the FSS analysis, much larger system sizes should be simulated. Alternatively, the fitting of the rescaling factor  $\lambda(L)$  should involve two exponents – the main one and  $\theta$ . This introduces significant uncertainty which requires large computational efforts to minimize the contributions of errors from several fitting parameters.

*Acknowledgments.* We acknowledge helpful discussions with Victor Bondarev, Alexander Patashinskii and Aleksey Tselik. This work was supported by the National Science Foundation under the grant PHY1314469.

- 
- <sup>1</sup> L.D. Landau and E. M. Lifshitz, *Statistical Physics. Volume 5*, Butterworth-Heinemann, 1980.
  - <sup>2</sup> L. P. Kadanoff, W. Götze, D. Hamblen, R. Hecht, E. A. S. Lewis, V. V. P. Ciauskas, M. Rayl, J. Swift, Rev. Mod. Phys. **39**, 395 (1967).
  - <sup>3</sup> A.Z. Patashinskii, and V.L. Pokrovsky, *Fluctuation Theory of Phase Transitions*, Elsevier (1979).
  - <sup>4</sup> T. D. Lee and C. N. Yang, Phys.Rev. **87**, 410(1952).
  - <sup>5</sup> N. D. Mermin, Phys.Rev.Lett. **26**, 169(1971); *ibid.* 957(1971).
  - <sup>6</sup> J. Rehr and N. Mermin, Phys. Rev. **A8**, 472 (1973).
  - <sup>7</sup> V. L. Pokrovskii, Pisma v ZhETF, **17**, 219 (1973).
  - <sup>8</sup> J. Hubbard and P. Schofield, Phys. Lett. **40A**, 245(1972).
  - <sup>9</sup> S.-K. Ma, *Modern Theory of Critical Phenomena*, W.A. Benjamin, Inc., London-Tokyo, 1976.
  - <sup>10</sup> O. T. Valls and J. A. Hertz, Phys. Rev. **B18**, 2367(1978).
  - <sup>11</sup> J. F. Nicoll, Phys. Lett. **76A**, 112(1980).
  - <sup>12</sup> V. N. Bondarev, Phys. Rev. **E 77**, 050103(R) (2008).
  - <sup>13</sup> V. N. Bondarev, private communication.
  - <sup>14</sup> V. P. Warkulwizt, B. Mozer, M. S. Green, Phys. Rev. Lett. **32**, 1410 (1974).
  - <sup>15</sup> C. W. Garland, J. Thoen, Phys. Rev. **A13**, 1601 (1976).
  - <sup>16</sup> C. E. Hayes and H. V. Carr, Phys. Rev. Lett. **39**, 1558 (1977).
  - <sup>17</sup> M. W. Pestak and M. H. W. Chan, Phys. Rev. **B 30**, 274 (1984).
  - <sup>18</sup> M. Barmatz, I. Hahn, J. A. Lipa, R. V. Duncan, Rev. Mod. Phys. **79**, 1 (2007).
  - <sup>19</sup> A. D. Bruce and N. B. Wilding, Phys. Rev. Lett. **68**, 193 (1992).
  - <sup>20</sup> N. B. Wilding, Phys. Rev. **E 52**, 602 (1995).
  - <sup>21</sup> G. Orkoulas and A. Z. Panagiotopoulos, J. Chem. Phys. **110**, 1581(1999).
  - <sup>22</sup> J. J. Potoff and A. Z. Panagiotopoulos, J. Chem. Phys. **112**, 6411(2000).
  - <sup>23</sup> G. Orkoulas, M. E. Fisher, and A. Z. Panagiotopoulos, Phys. Rev. **E 63**, 051507 (2001).
  - <sup>24</sup> Y. C. Kim, M. E. Fisher, and G. Orkoulas, Phys. Rev. **E 67**, 061506 (2003).
  - <sup>25</sup> Y. C. Kim and Michael E. Fisher, Phys. Rev. **68**, 041506 (2003).
  - <sup>26</sup> H. Watanabe, N. Ito, and Chin-Kun Hu, J. Chem. Phys. **136**, 204102(2012).
  - <sup>27</sup> A.B. Kuklov, N.V. Prokofev, B.V. Svistunov, M. Troyer, Ann. Phys., **321**, 1602 (2006).
  - <sup>28</sup> A. M. Tselik and A. B. Kuklov, New J. Phys., **14**, 115033 (2012).
  - <sup>29</sup> M. Rovere, D. W. Heerman, K. Binder, J. Phys.: Cond. Mat. **2**, 7009(1990).
  - <sup>30</sup> N.V. Prokof'ev, B.V. Svistunov, and I.S. Tupitsyn, Phys. Lett. A **238**, 253-259 (1998); JETP **87**, 310-321 (1998).